# Uniform Practical Asymptotic Stability for Position Control of Underwater Snake Robots

Amer Orucevic[1], Jan Tommy Gravdahl[1], Kristin Y. Pettersen[1] and Antoine Chaillet[2]

***Abstract*— In this paper, Lyapunov theory for uniform practical asymptotic stability (UPAS) is presented and utilized to solve the problem of position control of a planar underwater snake robot (USR). First, a precise definition of UPAS is presented, which imposes that, locally, all solutions converge to the origin up to a steady-state error that can be arbitrarily reduced by a convenient parameter tuning. Additionally, a sufficient condition for UPAS of a time-varying nonlinear system and a theorem for UPAS of cascaded systems are presented. These are then utilized to design controllers that stabilize the position of an USR when approaching from such a direction that the USR moves against the current. Results from numerical simulations are then investigated to validate the theoretical results.**

## I. INTRODUCTION

Our understanding of the oceans is crucial for meeting challenges such as food sufficiency, bio-diversity, renewable energy, transport, and access to minerals and other resources. To fully access the vast oceans we need efficient, autonomous marine robots. One promising approach is using underwater snake robots (USRs), which are autonomous underwater vehicles (AUVs) consisting of several slim segments connected by joints, allowing them to access narrow spaces while moving by mimicking an eel [1]. The advantage of this design is that it can access narrow spaces and interact with its environment in the same way as a traditional robotic manipulator arm.

Power delivery remains a challenge for AUVs. Battery constraints limit their operational time, while tethers would limit their operational area and autonomy. Improving the energy efficiency of these systems would be a significant step forward in our attempts to design efficient AUVs. We want to pursue the idea of achieving energy autonomy by utilizing the energy in waves, currents and other hydrodynamic effects such as wakes behind bluff bodies [2], [3]. To this end, we aim to develop a controller that allows the USR to hold a desired position with an undulatory motion, downstream from a bluff body. As a first step to achieving this, we present a controller that stabilizes the position of a planar-USR with an undulatory motion when moving against a time-varying current.

Various control strategies have been developed and studied for undulatory motion of snake robots. The line-of-sight (LOS) guidance control law is implemented for terrestrial snake robots [4]. However, this does not apply for USRs, due to environmental disturbances. This issue was later addressed in [5], where the integral line-of-sight (ILOS) guidance control law was proposed for USRs and proven to provide semi-global exponential stability, under the assumption that the forward velocity is always greater than the current. Stabilizing the position of the USR however, requires that these velocities are equal. Directional following control of the terrestrial snake robot is studied in [6], by using virtual holonomic constraints (VHCs) to encode a sinusoidal gait pattern for forward propulsion. This was done by utilizing hierarchical control design [7]. A similar approach was later used to design maneuvering controllers for both terrestrial snake robots [8] and USRs [9]. Our goal is for the USR to operate in the wake of a bluff body, where the environmental forces are time-varying, which results in reference signals and disturbances that are time dependent. The controllers developed [8], [9] however, assume that the systems are time-invariant. To address this issue, in this paper the control approach and corresponding stability proofs are extended to time-varying systems. Additionally, to achieve a desired orientation that drives the USR towards a reference position, a guidance law is proposed that generates a reference angular velocity. The controllers presented in [8], [9] are, however, designed for a desired heading angle. The controllers in this paper are therefore adapted for angular velocity tracking.

The guidance law proposed in this paper is inspired by the approaches taken in [10], [11] where a geometric controller is developed and studied for position tracking of quad-copters in three-dimensions. This was later adapted for path-following of underactuated autonomous surface vessels (ASVs) and planer AUVs [12]. For our purposes the guidance law has been adapted for position tracking of planar USRs, by including a reference velocity along the $y$-axis in addition to the reference velocity along the $x$-axis used in [12]. The reference velocities are then designed to stabilize the position of the USR.

We cannot use hierarchical control design [7], which the stability analysis in [6], [8], [9] is based on, as it requires time-invariant systems. Instead, we consider cascaded systems theory, which has proved to be an efficient tool for analyzing the stability of nonlinear dynamical systems [13], [14]. For time-varying nonlinear systems, cascaded systems theory is well established for cascades of uniformly asymptotically stable systems; uniformly globally asymptotically stable (UGAS) systems [14], uniformly semi-globally asymptotically stable (USAS) systems [15] and locally uni-

[1]A. Orucevic, J. T. Gravdahl, K. Y. Petttersen are with the Centre for Autonomous Marine Operations and Systems, Department of Engineering Cybernetics, Norwegian University of Science and Technology (NTNU), Trondheim, Norway {Amer.Orucevic, Tommy.Gravdahl, Kristin.Y.Pettersen}@ntnu.no

[2]A. Chaillet is with Laboratoire des Signaux et Systèmes, CentraleSupélec, Univ. Paris Saclay, Gif sur Yvette, France antoine.chaillet@centralesupelec.fr

formly asymptotically stable (UAS) systems [16].

However, the presence of non-vanishing perturbations such as modelling errors, unmodelled disturbances and measurement noise, asymptotic stability may not be attainable. In these cases the system may not converge to the origin but rather to some neighborhood of the origin. When that neighborhood can be diminished at will by the choice of parameters, this is referred to as uniform global practical asymptotic stability (UGPAS). In [15] it is shown that a cascaded system consisting of two UGPAS systems with uniformly bounded (UB) solutions retains the UGPAS property. Moreover, Lyapunov sufficient conditions for UGPAS are proposed and proven. The global requirements of UGPAS can be alleviated by considering uniform semi-global practical asymptotic stability (USPAS). This has been studied in [17] where Lyapunov sufficient conditions and stability of cascades of USPAS systems were proven. However, USPAS requires that the region of attraction can be enlarged to any desirable size by the choice of parameters. The guidance laws and controllers in [10]–[12] give almost-GAS and put constraints on the desired velocities of the vehicles, and therefore achieving either global or semi-global stability is not possible. The strongest stability property we may hope to establish for the resulting closed-loop system is thus local uniform practical asymptotic stability (UPAS). This is a special case of USPAS where the region of attraction is not required to be arbitrarily enlargeable. As Lyapunov and cascades systems theory for UPAS systems could not be found in literature, in this paper we establish both Lyapunov sufficient conditions for UPAS of time-varying nonlinear systems as well as for cascades of such systems. We then apply these to prove UPAS of the closed-loop system, proving that the proposed control law stabilizes the position of the USR with an undulatory motion in the presence of time-varying disturbances when moving against a constant current along the $x$-axis.

The paper is organized as follows: In Section II the notation used in this paper is presented. Then in Section III we present the precise definition of UPAS as we use it. Furthermore, a proposition for sufficient conditions for UPAS of a time-varying dynamical system and a theorem for UPAS of cascaded systems are presented. In Section IV the control objectives and a control oriented model of an USR are presented. The controllers and guidance law proposed in this paper are then presented in Section V, with an analysis of the resulting closed-loop system. Then the simulation setup and results are presented in Section VI. Finally, in Section VII conclusions are given.

## II. Notation

A class $\mathcal{K}$-function is a continuous function $\alpha : \mathbb{R}_{\geq 0} \to \mathbb{R}_{\geq 0}$ that is strictly increasing and satisfying $\alpha(0) = 0$. If additionally $\alpha(s) \to \infty$ when $s \to \infty$ then $\alpha \in \mathcal{K}_\infty$. A class $\mathcal{L}$-function is a continuous function $\sigma : \mathbb{R}_{\geq 0}$ that is non-increasing and $\sigma(s) \to 0$ when $s \to \infty$. A function $\beta : \mathbb{R}_{\geq 0} \times \mathbb{R}_{\geq 0} \to \mathbb{R}_{\geq 0}$ is said to be of class $\mathcal{KL}$ if $\beta(\cdot, t) \in \mathcal{K}$ for all $t \in \mathbb{R}_{\geq 0}$ and $\beta(s, \cdot) \in \mathcal{L}$ for all $s \in \mathbb{R}_{\geq 0}$. A closed ball of radius $\delta$ centered at the origin is denoted by $\mathcal{B}_\delta := \{x \in \mathbb{R}^n : |x| \leq \delta\}$ where $|\cdot|$ is the Euclidean norm. We define $|x|_\delta := \inf_{z\in\mathcal{B}_\delta} |x - z|$, and the subset $H(\delta, \Delta) := \{x \in \mathbb{R}^n \mid \delta \leq |x| \leq \Delta\}$. The definitions for UAS of a ball used in this paper are the same as presented in [17].

## III. Uniform Practical Asymptotic Stability

In this section we give a precise definition of UPAS, we provide Lyapunov sufficient conditions for UPAS, and we present results on the stability of cascaded systems consisting of UPAS sub-systems.

### A. UPAS definition

We consider parameterized time-varying dynamical systems on the following form:

$$\dot{x} = f(t, x, \theta), \tag{1}$$

where $x \in \mathbb{R}^n$, $t \in \mathbb{R}_{\geq 0}$, $\theta \in \mathbb{R}^m$ is a constant parameter, typically a control gain that can be tuned and $f : \mathbb{R}_{\geq 0} \times \mathbb{R}^n \times \mathbb{R}^m \to \mathbb{R}^n$ is locally Lipschitz in $x$ and piece-wise continuous in $t$ and $\theta$. An estimate of the domain of attraction is given by $D_f(a, b) := \{\theta \in \mathbb{R}^m \mid \mathcal{B}_a \text{ is UAS on } \mathcal{B}_b \text{ for (1)}\}$.

**Definition 1.** *(UPAS) Let $\Theta \subset \mathbb{R}^m$ be a set of parameters. The system (1) is said to be Uniformly Practically Asymptotically Stable (UPAS) on $\Theta$ if for some $\Delta > 0$, for any positive $\delta < \Delta$ there exists $\theta^*(\delta) \in \Theta$ such that the ball $\mathcal{B}_\delta$ is UAS on $\mathcal{B}_\Delta$ for the system (1).*

Note that this is a local adaptation of UGPAS and USPAS as presented in [15] and [17]. Specifically the radius $\Delta$ of $\mathcal{B}_\Delta$ can be increased arbitrarily by the choice of parameters, the definition extends to that of USPAS, and if $\Delta \to \infty$ regardless of the parameters selected, then it becomes the definition of UGPAS.

### B. Lyapunov sufficient conditions for UPAS

The following proposition is an adaptation of Theorem 10 in [17] and gives sufficient conditions for a system on the form (1) to be UPAS.

**Proposition 1.** *(Lyapunov sufficient conditions for UPAS) Suppose that there exists a $\Delta > 0$ such that, for any positive $\delta < \Delta$ there exist a parameter $\theta^*(\delta) \in \Theta$, a continuously differentiable function $V_\delta : \mathbb{R}_{\geq 0} \times \mathbb{R}^n \to \mathbb{R}_{\geq 0}$, and class $\mathcal{K}_\infty$-functions $\underline{\alpha}_\delta$, $\overline{\alpha}_\delta$ and $\alpha_\delta$, such that for all $x \in H(\delta, \Delta)$, and all $t \in \mathbb{R}_{\geq 0}$*

$$\underline{\alpha}_\delta(|x|) \leq V_\delta(t, x) \leq \overline{\alpha}_\delta(|x|), \tag{2}$$

$$\frac{\partial V_\delta}{\partial t}(t, x) + \frac{\partial V_\delta}{\partial x}(t, x) f(t, x, \theta^*) \leq -\alpha_\delta(|x|), \tag{3}$$

$$\lim_{\delta\to 0} \underline{\alpha}_\delta^{-1} \circ \overline{\alpha}_\delta(\delta) = 0. \tag{4}$$

*then the system (1) is UPAS on the parameter set $\Theta$.*

*Proof:* The proof follows directly from the proof of Theorem 10 in [17] by setting $\Delta_1$ to be constant.

It is worth stressing that the $K_\infty$ functions involved in (2) - (3) typically depend on the the value of the parameter $\theta$, which is itself tuned to reach a given steady-state precision

$\delta$. In other words, these $K_\infty$ functions typically depend on $\delta$, as witnessed by the subscript. This is what makes condition (4) non-trivial.

### C. UPAS of cascades

We consider the cascaded system

$$\dot{x}_1 = f_1(t, x_1, \theta_1) + g(t, x, \theta)x_2, \tag{5a}$$

$$\dot{x}_2 = f_2(t, x_2, \theta_2), \tag{5b}$$

where $x := [x_1^T, x_2^T]^T \in \mathbb{R}^{n_1} \times \mathbb{R}^{n_2}$ are the states, $\theta := [\theta_1^T, \theta_2^T]^T \in \mathbb{R}^{m_1} \times \mathbb{R}^{m_2}$ are the parameters, $t \in \mathbb{R}_{\geq 0}$, $f_1$, $f_2$ and $g$ are locally Lipschitz in the states and parameters, and piece-wise continuous in time. To establish UPAS of cascaded systems on the form given by (5), an adaptation of Theorem 13 in [17] is made. The following assumptions are made:

**Assumption 1.** *(UPAS of the driving subsystem) The driving system (5b) is UPAS on $\Theta_2$.*

**Assumption 2.** *(UPAS of the driven subsystem) For some $\Delta_1 > 0$ and any $\delta_1$ such that $\Delta_1 > \delta_1 > 0$, there exist a parameter $\theta_1^*(\delta_1) \in \Theta_1$, a continuously differentiable function $V_{\delta_1}$, and class $\mathcal{K}_\infty$ functions $\underline{\alpha}_{\delta_1}$, $\overline{\alpha}_{\delta_1}$ and $\alpha_{\delta_1}$ such that conditions* (2). (3) *and* (4) *are satisfied with these functions, and a continuous positive non-decreasing function $c_{\delta_1}$ exists such that for all $x_1 \in H(\delta_1, \Delta_1)$ and all $t \in \mathbb{R}_{\geq 0}$*

$$\left| \frac{\partial V_{\delta_1}}{\partial x_1}(t, x_1) \right| \leq c_{\delta_1}(|x_1|). \tag{6}$$

**Assumption 3.** *(Boundedness of the interconnection term) The function $g$ is uniformly bounded both in time and parameters, i.e there exists a non-decreasing function $G : \mathbb{R}_{\geq 0} \to \mathbb{R}_{\geq 0}$ such that, for all $x \in \mathbb{R}^{n_1} \times \mathbb{R}^{n_2}$, all $\theta \in \Theta_1 \times \Theta_2$ and all $t \in \mathbb{R}_{\geq 0}$*

$$|g(t, x, \theta)| \leq G(|x|). \tag{7}$$

**Assumption 4.** *(Boundedness of solutions) There exists a positive constant $\Delta_0$ such that there exist positive numbers $\Delta_1 > max\{\delta_1, \Delta_0\}$ and $\Delta_2 > \delta_2$, and parameter $\theta_1^*(\delta_1)$ as defined in Assumption 2, there exists a parameter $\theta_2^* \in D_{f_2}(\delta_2, \Delta_2) \cap \Theta_2$, and a continuous function $\gamma(a, b) : \mathbb{R}_{\geq 0} \times \mathbb{R}_{\geq 0} \to \mathbb{R}_{\geq 0}$ such that the trajectories of* (5) *with $\theta = \theta^*$ satisfy*

$$|x_0| \leq \gamma(\Delta_1, \Delta_2) \Longrightarrow |x(t, t_0, x_0, \theta^*)| \leq \Delta_1, \ \forall t \geq t_0 \tag{8}$$

**Theorem 1.** *Under Assumptions 1-4 the cascaded system (5) is UPAS on $\Theta_1 \times \Theta_2$.*

*Proof:* The proof follows directly from the proof of Theorem 13 in [17] by setting $\Delta_1$ to be constant.

## IV. Control oriented model

A detailed model of an USR where the full kinematics and dynamics of a planar snake robot with revolute joints are considered, is presented in [18]. The closed-loop form of this model is validated through experiments, and the results are used in a comparison between experiments and simulations for path following in [1]. The complexity of this model makes it less appropriate for the design of control systems and motion planning. A simplified control-oriented model was thus developed in [19], and later extended to USRs in [20]. The model was developed further in [21], where constant ocean currents were added. The control-oriented model was later used to develop a controller for integral line-of-sight guidance, and the controller was validated through experiments in [22]. In this paper we modify the current that is parallel to the $y$-axis to be time-varying. The control-oriented model is then given by:

$$\dot{\boldsymbol{\phi}} = \boldsymbol{v}_\phi, \tag{9a}$$

$$\dot{\eta} = r, \tag{9b}$$

$$\dot{p}_x = v_t \cos\eta - v_n \sin\eta + V_x, \tag{9c}$$

$$\dot{p}_y = v_t \sin\eta + v_n \cos\eta + V_y(t), \tag{9d}$$

$$\dot{\boldsymbol{v}}_\phi = -\frac{c_n}{m}\boldsymbol{v}_\phi + \frac{c_p}{m} v_t \boldsymbol{A}\boldsymbol{D}^T\boldsymbol{\phi} + \frac{1}{m}\boldsymbol{D}\boldsymbol{D}^T\boldsymbol{u}, \tag{9e}$$

$$\dot{r} = -\lambda_1 r + \frac{\lambda_2}{N_l - 1} v_t \bar{\boldsymbol{e}}^T\boldsymbol{\phi}, \tag{9f}$$

$$\begin{aligned}\dot{v}_t = &-\frac{c_t}{m}v_t + \frac{2c_p}{N_l m}\bar{\boldsymbol{e}}^T\boldsymbol{\phi}v_n - \frac{c_p}{N_l m}\boldsymbol{\phi}^T\boldsymbol{A}\bar{\boldsymbol{D}}\boldsymbol{v}_\phi \\ &+ r(V_x \sin\eta - V_y(t)\cos\eta) - \dot{V}_y(t)\sin\eta,\end{aligned} \tag{9g}$$

$$\begin{aligned}\dot{v}_n = &-\frac{c_n}{m}v_n + \frac{2c_p}{N_l m}\bar{\boldsymbol{e}}^T\boldsymbol{\phi}v_t \\ &+ r(V_x \cos\eta + V_y(t)\sin\eta) - \dot{V}_y(t)\cos\eta.\end{aligned} \tag{9h}$$

Here $\boldsymbol{\phi}$ contains all the relative $N_l - 1$ joint angles $\phi_i$ while $\eta$ denotes the heading of the snake robot. The position of the USR is given by $[p_x, p_y]^T$. The angular velocity of the joints is given by $\boldsymbol{v}_\phi$, while the angular velocity of the heading is given by $r$. The velocities relative to the ocean current are given by $v_t$ and $v_n$, respectively. Additionally, current velocity is given by $[V_x, V_y(t)]^T$, where $V_y(t)$ is time-varying and bounded. Additionally we define $|V_\alpha|$ as the bound of $V_y(t)$. Furthermore, $\lambda_i$ are constants that characterize the rotational dynamics. The $c_t, c_n$ coefficients are the drag coefficients in the tangential and normal directions, respectively, while $c_p$ is the propulsion coefficient. The summation vector is denoted as $\bar{\boldsymbol{e}} = [1, \ ..., \ 1]^T \in \mathbb{R}^{N_l - 1}$, and the matrix $\bar{\boldsymbol{D}} = \boldsymbol{D}^T(\boldsymbol{D}\boldsymbol{D}^T)^{-1}$. The $\boldsymbol{A}$ and $\boldsymbol{D}$ are given by $\boldsymbol{D} = \begin{bmatrix} 1 & -1 & & \\ & \ddots & \ddots & \\ & & 1 & -1 \end{bmatrix}$, $\boldsymbol{A} = \begin{bmatrix} 1 & 1 & & \\ & \ddots & \ddots & \\ & & 1 & 1 \end{bmatrix}$.

## V. Control design

### A. Control objectives and approach

The approach presented in this paper is inspired by [8], [9], [12]. However, because the proposed controller is designed to handle time-varying references and disturbances, the hierarchical approach as used in these papers can not be used in our control design and analysis. Instead a cascaded system approach [14] based on the results of Section III will be utilized.

The control objective is to achieve a desired position downstream from a bluff body. The vortexes that are shed from the bluff body result in a sinusoidal motion induced through the USR. Therefore, to take advantage of this energy, it is preferable that the USR moves in a similar sinusoidal pattern. The controllers presented in [9] use such a sinusoidal gait to achieve forward propulsion while also achieving a desired velocity and orientation. Therefore, in this paper we choose to use the same sinusoidal gate as presented in previous work, where each of the joints is given by $i$,

$$\phi_{d,i} = \alpha\gamma_1(i)\sin(\lambda + (i-1)\delta) + g_2(\phi_0), \qquad (10)$$

where $\alpha$ is the amplitude, $\gamma_1(i)$ is a scaling function that varies the amplitude along the snake body, and $\delta$ is the phase shift between adjacent joints. The variables $\lambda$ and $\phi_0$ are the frequency and turning parameters. A saturation function $g_2$ is designed to be strictly increasing and twice differentiable in the range $[\phi_{0,\min}, \phi_{0,\max}]$. The frequency and turning parameters will be treated as virtual control inputs and their references will be given by a guidance law, designed such that tracking these time-varying references leads to the desired position being acquired. Additionally we assemble all the reference signals into a vector $\boldsymbol{\phi}_d \in \mathbb{R}^{N_l-1}$.

### B. Joint controller

To achieve the desired relative angles, the following feedback linearizing controller is proposed

$$\boldsymbol{u} = m(\boldsymbol{D}\boldsymbol{D}^T)^{-1}[\frac{c_n}{m}\boldsymbol{v}_\phi - \frac{c_p}{m}v_t\boldsymbol{A}\boldsymbol{D}^T\boldsymbol{\phi} + \bar{\boldsymbol{u}}]. \qquad (11)$$

We choose $\bar{\boldsymbol{u}} = \ddot{\boldsymbol{\phi}}_d - K_{\phi,1}\dot{\tilde{\boldsymbol{\phi}}} - K_{\phi,2}\tilde{\boldsymbol{\phi}}$, where $K_{\phi,1}$, $K_{\phi,2} > 0$, and $\tilde{\boldsymbol{\phi}} = \boldsymbol{\phi} - \boldsymbol{\phi}_d$.

**Proposition 2.** *Consider a USR described by (9), then the controller (11) ensures that for the system* (9) *that* $\tilde{\phi}$ *converges to zero exponentially fast.*

*Proof:* Inserting (11) into (9e) yields

$$\ddot{\tilde{\boldsymbol{\phi}}} + K_{\phi,1}\dot{\tilde{\boldsymbol{\phi}}} + K_{\phi,2}\tilde{\boldsymbol{\phi}} = 0, \qquad (12)$$

which is uniformly globally exponentially stable (UGES).

### C. Velocity controller

To achieve a desired relative velocity, equation (9g) is rewritten by using (10), giving

$$\begin{aligned}\dot{v}_t = &-\frac{c_t}{m}v_t + X_n v_n - X_\lambda\dot{\lambda} - X_\phi\dot{\phi}_0 - \dot{V}_y(t)\sin\eta \\ &+ r[V_x\sin\eta - V_y(t)\cos\eta]) + g_1(t,\tilde{\boldsymbol{\phi}},\dot{\tilde{\boldsymbol{\phi}}}),\end{aligned} \qquad (13a)$$

where we define $\bar{\boldsymbol{B}} := \boldsymbol{A}\bar{\boldsymbol{D}}$ and

$$g_1(t,\tilde{\boldsymbol{\phi}},\dot{\tilde{\boldsymbol{\phi}}}) := -\frac{c_p((2\tilde{\boldsymbol{\phi}} + \boldsymbol{\phi}_d)^T\bar{\boldsymbol{B}}\dot{\tilde{\boldsymbol{\phi}}} + \dot{\tilde{\boldsymbol{\phi}}}^T\bar{\boldsymbol{B}}\dot{\boldsymbol{\phi}}_d)}{N_l m}, \qquad (14a)$$

$$X_\phi := \frac{c_p}{N_l m}\boldsymbol{\phi}_d^T\bar{\boldsymbol{B}}, \qquad (14b)$$

$$X_\lambda := X_\phi\alpha[\cos(\lambda) + ... + \cos(\lambda + \delta(N_l - 1))]. \qquad (14c)$$

Furthermore, we define the error variables $z_1 := v_t - V_d$ and $z_2 := \dot{\lambda} - \zeta_1$, where $V_d$ is the reference tangential relative velocity and $\zeta_1$ is a virtual control input, which is used to stabilize $z_1$. To achieve the desired velocity, we propose a backstepping controller. We define $\boldsymbol{\psi}_1$ such that:

$$\begin{aligned}\dot{z}_1 = &-\frac{c_t}{m}v_t + \psi_1(t, v_n, v_\theta, \eta) - X_\phi\dot{\phi}_0 \\ &- X_\lambda(\zeta_1 + z_2) + g_1(\tilde{\boldsymbol{\phi}}, \dot{\tilde{\boldsymbol{\phi}}}),\end{aligned} \qquad (15)$$

and choose the virtual input as

$$\zeta_1 = \frac{-\frac{c_t}{m}V_d - \boldsymbol{\psi}_1(t, v_n, v_\theta, \eta) - X_\phi\dot{\phi}_0 + K_{\lambda,1}z_1}{X_\lambda}, \qquad (16a)$$

$$\zeta_1 = \frac{\zeta_1^* - X_\phi\dot{\phi}_0}{X_\lambda}. \qquad (16b)$$

The derivative of the second error variable $z_2$ is the found as

$$\dot{z}_2 = u_\lambda - \frac{\dot{\zeta}_1^*}{X_\lambda} + \frac{\dot{X}_\lambda(\zeta_1^* + X_\phi\dot{\phi}_0)}{X_\lambda^2} - \frac{X_\phi\ddot{\phi}_0 + \dot{X}_\phi\dot{\phi}_0}{X_\lambda}. \qquad (17)$$

The control input is then selected as

$$u_\lambda = \frac{\dot{\zeta}_1^* + \dot{X}_\phi\dot{\phi}_0}{X_\lambda} - \frac{\dot{X}_\lambda(\zeta_1^* + X_\phi\dot{\phi}_0)}{X_\lambda^2} - K_{\lambda,2}z_2 + X_\lambda z_1. \qquad (18)$$

By inserting the virtual input (16) and the control input (18), the closed-loop system is then given by

$$\dot{z}_1 = -\left(\frac{c_t}{m} + K_{\lambda,1}\right)z_1 - X_\lambda z_2 + g_1(t,\tilde{\phi},\dot{\tilde{\phi}}), \qquad (19a)$$

$$\dot{z}_2 = -K_{\lambda,2}z_2 + X_\lambda z_1 + \frac{X_\phi}{X_\lambda}u_\phi. \qquad (19b)$$

We define the paramterset $\boldsymbol{\varphi}_1 := [\boldsymbol{\varphi}_2, \boldsymbol{\varphi}_3]^T$, where $\boldsymbol{\varphi}_2 := [K_{\phi,1}, K_{\phi,2}]^T$ and $\boldsymbol{\varphi}_3 := [K_{\lambda,1}, K_{\lambda,2}]^T$.The cascaded system can then be written as

$$\dot{\boldsymbol{x}}_1 = \boldsymbol{f}_1(t, \boldsymbol{x}_1, \boldsymbol{x}_2, \boldsymbol{\varphi}_2) + \boldsymbol{g}_\lambda(t, \boldsymbol{x}_2)\boldsymbol{x}_2, \qquad (20a)$$

$$\dot{\boldsymbol{x}}_2 = \boldsymbol{f}_2(\boldsymbol{x}_2, \boldsymbol{\varphi}_3), \qquad (20b)$$

where we define $\boldsymbol{x}_1 := [z_1, z_2]^T$ and $\boldsymbol{x}_2 := [\tilde{\boldsymbol{\phi}}, \dot{\tilde{\boldsymbol{\phi}}}]^T$. The dynamics and interconnection-term are given by (12), (19) and (14a).

**Proposition 3.** *The cascaded system (20), with the backstepping controller (18) is UPAS on* $\boldsymbol{\varphi}_1$ *and the solutions are globally uniformly bounded (GUB).*

*Proof:* Consider the Lyapunov function defined as $V_1 := (1/2)z_1^2 + (1/2)z_2^2$. From Proposition 2 it is known that $\boldsymbol{x}_2$ is bounded. Furthermore, the references $\boldsymbol{\phi}_d$ and $\dot{\boldsymbol{\phi}}_d$ are bounded by design. This implies that $g_1$, $X_\phi$ and $X_\lambda$ are bounded. We denote the bounds by $g_{1,m}$, $X_{\phi,m}$ and $X_{\lambda,m}$. The following is then derived:

$$\begin{aligned}\dot{V}_1 \leq &-\left[\left(\frac{c_t}{m} + K_{\lambda,1}\right)|z_1| - g_{1,m}\right]|z_1| \\ &-\left(K_{\lambda,2}|z_2| - \frac{X_{\phi,m}}{X_{\lambda,m}}u_{\phi,m}\right)|z_2|,\end{aligned} \qquad (21)$$

where $u_{\phi,m}$ is the bound of the angular velocity control input. The derivative (21) is negative definite for

$$|\boldsymbol{x}_1| > \frac{g_{1,m}}{\frac{c_t}{m} + K_{\lambda,1}} + \frac{X_{\phi,m}}{X_{\lambda,m}K_{\lambda,2}}|u_{\phi,m}|. \qquad (22)$$

This means that $\boldsymbol{x}_1$ is GUB by Theorem 4.18 in [23]. The nominal system can be shown to be UPAS from (21), and the interconnection term is bounded.

Finally it is established in Proposition 2 that the driving system is UGES. Then by Theorem 1 the system is UPAS on the set of parameters.

*D. Guidance law and attitude controller*

The guidance law presented in this paper is inspired by [10]–[12]. The planar geometric path following law is modified to include a desired velocity $u_y$ along the $y$-axis in addition to the velocity $u_x$ along the $x$-axis. The velocity references will be designed to stabilize the position of the USR. To drive the USR towards a reference position, a desired orientation is defined as

$$\boldsymbol{R_d} := \begin{bmatrix} \frac{u_x - V_x}{\sqrt{N}} & \frac{u_y}{\sqrt{N}} \\ -\frac{u_y}{\sqrt{N}} & \frac{u_x - V_x}{\sqrt{N}} \end{bmatrix}, \tag{23}$$

where $N = (u_x - V_x)^2 + (u_y)^2$. This is illustrated in Figure 1 below. To design an attitude controller that drives the USR towards the desired orientation, an error function $\Psi(\boldsymbol{R}, \boldsymbol{R_d})$ is defined as

$$\Psi(\boldsymbol{R}, \boldsymbol{R_d}) := \frac{1}{2}\text{tr}[I - \boldsymbol{R_d}^T \boldsymbol{R}]. \tag{24}$$

Furthermore, the derivative of $\Psi$ with respect to $\boldsymbol{R}$ is defined as $\boldsymbol{D}_R \Psi(\boldsymbol{R}, \boldsymbol{R_d}) := e_R$, where $e_R$ is given by

$$\begin{bmatrix} 0 & -e_R \\ e_R & 0 \end{bmatrix} = \frac{1}{2}(\boldsymbol{R_d}^T \boldsymbol{R} - \boldsymbol{R}^T \boldsymbol{R_d}). \tag{25}$$

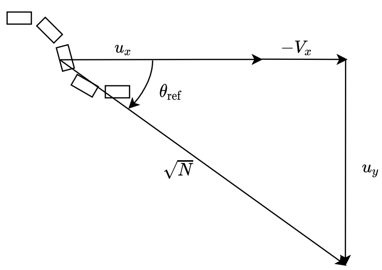


Fig. 1: Geometric representation of guidance law.

The desired angular velocity is found to be [12]

$$\begin{bmatrix} 0 & -r_d \\ r_d & 0 \end{bmatrix} = \boldsymbol{R_d}^T \dot{\boldsymbol{R}}_{\boldsymbol{d}}. \tag{26}$$

By defining $y_1 := r - r_d$ and the choice of $r_d$ given by (26) the following can be found

$$\frac{d\Psi(\boldsymbol{R}, \boldsymbol{R_d})}{dt} = e_R y_1, \tag{27a}$$

$$\dot{e}_r = C y_1, \tag{27b}$$

where $|C| \leq 1$. The error function $\Psi(\boldsymbol{R}, \boldsymbol{R_d}) \in [0, 2]$, where $\Psi(\boldsymbol{R}, \boldsymbol{R_d}) = 0$ implies that the heading of the USR is aligned with the desired orientation, while $\Psi(\boldsymbol{R}, \boldsymbol{R_d}) = 2$ implies that the USR is pointed in the opposite direction of the desired orientation. From (25) we see that $e_R = 0$ when $\boldsymbol{R} = \boldsymbol{R_d}$ and $\boldsymbol{R} = -\boldsymbol{R_d}$, implying that there are two equilibrium points in the dynamics of the orientation.

Motivated by [11], [12] we define the subset level $L_2 := \{\boldsymbol{R} \in SO(2) | \Psi(\boldsymbol{R}, \boldsymbol{R}_d) < 2\}$. The attitude controller is designed to ensure that given some initial conditions, $\boldsymbol{R}$ always lies in $L_2$. The error dynamics are defined as $y_2 := g_2(\phi_0) - \chi_1$, $y_3 := \dot{\phi}_0 - \chi_2$, where $\chi_1$ and $\chi_2$ are virtual inputs.

We define the interconnection term and sinusoidal gate

$$g_3(t, \tilde{\boldsymbol{\phi}}, z_1) := \frac{\lambda_2}{N_l - 1}((z_1 + V_d)\bar{e}^T \tilde{\boldsymbol{\phi}} + z_1 \bar{e}^T \boldsymbol{\phi}_d), \tag{28a}$$

$$\alpha_1(\lambda) := \alpha[\sin(\lambda), ..., \sin(\lambda + \delta(N_l - 1))]^T. \tag{28b}$$

The virtual inputs and real input are then selected as

$$\chi_1 = \frac{\lambda_1 r_d - \lambda_2 V_d \alpha(\lambda) - \dot{r}_d - K_1 z_1 - K_R e_R}{\lambda_2 V_d}, \tag{29a}$$

$$\chi_2 = \frac{1}{\partial g(\phi_0)/\partial \phi_0} \left[\dot{\chi}_1 - \lambda_2 V_d y_1 - K_2 y_2\right], \tag{29b}$$

$$u_\phi = \dot{\chi}_2 - \frac{\partial g(\phi_0)}{\partial \phi_0} y_2 - K_3 y_3. \tag{29c}$$

This gives the following closed loop dynamics

$$\begin{aligned} \dot{y}_1 = &-(\lambda_1 + K_1) y_1 + \lambda_2 V_d y_2 \\ &- K_R e_R + g_3(t, \tilde{\boldsymbol{\phi}}, z_1), \end{aligned} \tag{30a}$$

$$\dot{y}_2 = \frac{\partial g_2(\phi_0)}{\partial \phi_0} y_3 - \lambda_2 V_d y_1 - K_2 y_2, \tag{30b}$$

$$\dot{y}_3 = -\frac{\partial g_2(\phi_0)}{\partial \phi_0} y_2 - K_3 y_3. \tag{30c}$$

We define $\boldsymbol{x}_3 := [e_R, y_1, y_2, y_3]^T$, $\boldsymbol{x}_4 := [\boldsymbol{x}_1, \boldsymbol{x}_2]^T$, $\boldsymbol{\varphi}_4 = [K_1, K_2, K_3, K_R]^T$, $\boldsymbol{\varphi}_5 = [\boldsymbol{\varphi}_4, \boldsymbol{\varphi}_1]^T$ and the initial states $y_{i0}$. We then have the following cascaded system

$$\dot{\boldsymbol{x}}_3 = \boldsymbol{f}_3(t, \boldsymbol{x}_3, \boldsymbol{\varphi}_4) + \boldsymbol{g}_3(t, \boldsymbol{x}_4), \tag{31a}$$

$$\dot{\boldsymbol{x}}_4 = \boldsymbol{f}_4(t, \boldsymbol{x}_4, \boldsymbol{\varphi}_1), \tag{31b}$$

where $\boldsymbol{f}_3$, $\boldsymbol{g}_3$ and $\boldsymbol{f}_4$ are given by (30), (27) and (20). The following proposition can then be made:

**Proposition 4.** *Consider a system with dynamics (9) and controller (29), and suppose that the initial conditions satisfy*

$$\Psi(\boldsymbol{R}(0), \boldsymbol{R}_d(0)) < 2, \tag{32a}$$

$$y_{10}^2 + y_{20}^2 + y_{30}^2 < 2K_R(2 - \Psi(\boldsymbol{R}(0), \boldsymbol{R}_d(0))). \tag{32b}$$

*Then, for sufficiently small values of* $\tilde{\phi}$ *and* $z_1$*, and by selecting* $K_1$ *such that*

$$\frac{g_{3,m}}{(\lambda_1 + K_1)} << 2K_R \tag{33}$$

*it can be shown that* $\Psi(\boldsymbol{R}(0), \boldsymbol{R}_d(0)) \in L_2 \ \forall t$.

*Proof:* We define $V_2 := \frac{1}{2}y_1^2 + \frac{1}{2}y_2^2 + \frac{1}{2}y_3^2 + K_R \Psi(\boldsymbol{R}, \boldsymbol{R_d})$. To ensure that $\Psi(\boldsymbol{R}(t), \boldsymbol{R}_d(t)) < 2$ the derivative of $V_3$ has to be negative definite when approaching the ball $\beta_r$ where $r = 2K_R$. From Proposition 3 it is shown that $z_1$ is bounded. Furthermore $V_d$ is bounded by design. We define $g_{3,m}$ and $V_m$ as the bound of the interconnection term and desired relative tangential velocity, respectively. Then the following bound is found for the derivative of the Lyapunov function

$$\begin{aligned} \dot{V}_2 \leq &-(\lambda_1 + K_1)|y_1|^2 - K_2|y_2|^2 - K_3|y_3|^2 \\ &+ g_{3,m}|y_1|. \end{aligned} \tag{34}$$

By selecting the gains as in (33), the Lyapunov function is negative definite when approaching a circle with radius $2K_R$, implying that if the initial values satisfy (32) the states are bounded away from $\beta_r \ \forall t$.

We define $\lambda_m$ and $\lambda_M$ as the smallest and largest eigenvalues, respectively.

**Proposition 5.** *Consider a system with dynamics (9) and the controller given by (29) and assume that the bounds given by (33) are satisfied and that*

$$K_2 > \frac{\lambda_2 V_m}{2,} \tag{35a}$$

$$\lambda_m(\boldsymbol{M}_{3,\phi}) > \frac{\lambda_2 V_m}{2}. \tag{35b}$$

*Then* (31a) *is UAS and the cascaded system given by (31) is UPAS on* $\boldsymbol{\varphi}_5$.

*Proof:* To show stability for the attitude dynamics, the following bounds are used

$$\frac{1}{2}||e_R||^2 \leq \Psi(\boldsymbol{R}, \boldsymbol{R}_d) \leq \frac{1}{2-\psi_\phi}||e_R||^2, \tag{36}$$

where $\Psi(\boldsymbol{R}, \boldsymbol{R}_d) \leq \psi_\phi < 2$, which is derived and proven in [11]. A new Lyapunov function is defined as $V_3 := V_2 + \frac{1}{2}\beta_\phi e_R y_1$, where $\beta_\phi$ is a positive constant. By using the bounds (36), it can be shown that the Lyapunov function is bounded by

$$\boldsymbol{x}_3^T \boldsymbol{M}_{\phi,1} \boldsymbol{x}_3 \leq V_3 \leq \boldsymbol{x}_3^T \boldsymbol{M}_{\phi,2} \boldsymbol{x}_3, \tag{37}$$

where $\boldsymbol{M}_{\phi,1} = \frac{1}{2}\begin{bmatrix} K_R & -\beta_\phi & 0 & 0 \\ -\beta_\phi & 1 & 0 & 0 \\ 0 & 0 & 1 & 0 \\ 0 & 0 & 0 & 1 \end{bmatrix}$, $\boldsymbol{M}_{\phi,2} = \frac{1}{2}\begin{bmatrix} \frac{2K_R}{2-\psi_\phi} & \beta_\phi & 0 & 0 \\ \beta_\phi & 1 & 0 & 0 \\ 0 & 0 & 1 & 0 \\ 0 & 0 & 0 & 1 \end{bmatrix}$. Selecting $\beta_\phi < \sqrt{K_R}$, the eigenvalues of $\boldsymbol{M}_{\phi,1}$ and $\boldsymbol{M}_{\phi,2}$ are positive, and the following bounds can be used

$$\lambda_m(\boldsymbol{M}_{\phi,1})||\boldsymbol{x}_3||^2 \leq V_3 \leq \lambda_M(\boldsymbol{M}_{\phi,2})||\boldsymbol{x}_3||^2, \tag{38}$$

We consider the nominal dynamics of (30), and find the following bound for $\dot{V}_3$

$$\begin{aligned} \dot{V}_3 \leq -\boldsymbol{x}_5^T &\begin{bmatrix} \beta_\phi K_R & -\frac{\beta_\phi(\lambda_1+K_1)}{2} \\ -\frac{\beta_\phi(\lambda_1+K_1)}{2} & ((\lambda_1+K_1)-\beta_\phi) \end{bmatrix} \boldsymbol{x}_5 \\ &- K_2 y_2^2 - K_3 y_3^2 + \lambda_2 V_d y_2 e_R, \end{aligned} \tag{39}$$

where $\boldsymbol{x}_5 = [\,|e_R| \;\; |y_1|\,]^T$. By selecting

$$\beta_\phi < \min\left\{(\lambda_1 - K_1), \frac{4K_R(\lambda_1+K_1)}{4K_R + (\lambda_1+K_1)^2}, \sqrt{K_R}\right\}, \tag{40}$$

the matrix in (39), which we denote as $\boldsymbol{M}_{\phi,3}$, is positive definite. Using Young's inequality [24] the bound can be rewritten as

$$\begin{aligned} \dot{V}_3 \leq &-\lambda_m(\boldsymbol{M}_{\phi,3})|y_1|^2 - (K_2 - \frac{\lambda_2 V_d}{2})y_2^2 \\ &- K_3 y_3^2 - (\lambda_m(\boldsymbol{M}_{\phi,3}) - \frac{\lambda_2 V_d}{2})|e_R|^2. \end{aligned} \tag{41}$$

The bound is negative definite if (35) are satisfied. This implies that $\boldsymbol{x}_3$ is UAS. Additionally all the conditions of Theorem 1 are satisfied and the cascaded system is UPAS on the set of parameters.

### *E. Position and sway velocity stabilization*

Motivated by [5], the point which defines the position of the robot is moved by a distance $\epsilon = -2(N-1)c_p/N_l m\lambda_2$. The new coordinates are given by

$$\dot{\bar{e}}_x = v_t \cos\eta - \bar{v}_n \sin\eta + V_x, \tag{42a}$$

$$\dot{\bar{e}}_y = v_t \sin\eta + \bar{v}_n \cos\eta + V_y(t), \tag{42b}$$

$$\dot{\bar{v}}_n = X(\eta)r - Y\bar{v}_n - \dot{V}_y(t)\cos\eta, \tag{42c}$$

where $\bar{e}_x$ and $\bar{e}_y$ are the position errors along the $x$ and $y$ -axis. Furthermore, $X(\eta) = \epsilon(c_n/m - \lambda_1) + V_x\cos\eta + V_y(t)\sin\eta$, and $Y = c_n/m$. We define $\boldsymbol{\varphi}_6 = [Y, \boldsymbol{\varphi}_5]^T$.

**Proposition 6.** *Consider the USR described by* (9)*, with the controllers* (11)*,* (18)*,* (29) *and the guidance law given in Section V-D. Then the transformed sway velocity* $\bar{v}_n$ *is GUB and the cascaded system is UPAS on* $\boldsymbol{\varphi}_6$.

*Proof:* We consider (42c) and rewrite the equation to

$$\dot{\bar{v}}_n = X(\eta)r_d - Y\bar{v}_n + X(\eta)y_1 - \dot{V}_y(t)\cos\eta. \tag{43}$$

We define $V_4 := (1/2)\bar{v}_n^2$, and the derivative is bounded by

$$\dot{V}_4 \leq -Y\bar{v}_n^2 + (|V_\alpha| + |X_M|(|r_d| + |y_1|))|\bar{v}_n|, \tag{44}$$

where $X_M = (|X| + |V_x| + |V_\alpha|)$. From Proposition 5 it is shown that $y_1$ is bounded. Furthermore $r_d$ is bounded by design. We define the upper limit of $y_1 + r_d$ as $r_M$. By inserting this we get

$$\dot{V}_4 \leq -Y\bar{v}_n^2 + (|V_\alpha| + 2|X_M||r_M|)|\bar{v}_n|, \tag{45}$$

which is negative definite for $|\bar{v}_n| > (|V_\alpha| + 2|X_M||r_M|)/Y$ and therefore uniformly bounded by Theorem 4.18 in [23]. Additionally the nominal system is UPAS by Proposition 1. The conditions of Theorem 1 are satisfied, and the cascaded system is UPAS on $\boldsymbol{\varphi}_6$.

To stabilize the position of the USR, it is necessary that the guidance law is well defined, that is $\sqrt{N} \neq 0$. The control inputs for the position are selected as $u_x = -ke_x$ and $u_y = -ke_y$. Additionally it is assumed that $(-ke_x - V_x) > 0$, which implies that the USR always approaches the desired position from such a direction that the current component along the $x$-axis runs towards the USR. Additionally the desired relative velocity is selected as $V_d = \sqrt{N}$.

Our goal is to design a controller that stabilizes the USR at some desired position close to a bluff body. For efficient movement and energy harvesting purposes this would be downstream in the wake of an object. Therefore the assumption that the USR moves against the current is reasonable. We define $\tilde{\eta} := \eta - \eta_d$ and $\boldsymbol{\varphi}_7 = [k, \boldsymbol{\varphi}_6]^T$.

**Proposition 7.** *Consider an USR described by* (9)*, with the controllers* (11)*,* (18)*,* (29) *and the guidance law given in Section V-D. Furthermore, assume that the USR is moving against the current component along the* $x$*-axis, such that* $(-ke_x - V_x) > 0$. *Additionally, assume the attitude error* $\tilde{\eta}$ *is small and bounded such that*

$$(1 - \frac{|\tilde{\eta}|^2}{2}) > 0. \tag{46}$$

*Then the position errors* $|e_x|$ *and* $|e_y|$ *are GUB and the cascaded system is UPAS on* $\boldsymbol{\varphi}_7$.

*Proof:* Consider the dynamics of the position errors (42). Furthermore assume that the attitude error $\tilde{\eta}$ is small so that $\cos\tilde{\eta} \approx (1 - \tilde{\eta}^2/2)$ and $\sin\tilde{\eta} \approx \tilde{\eta}$. We define $V_5 :=$

$(1/2)\bar{e}_x^2 + (1/2)\bar{e}_y^2$ and the following bound can be found

$$\begin{aligned} |\dot{V}_5| \leq & -k\left(1 - \frac{\tilde{\eta}^2}{2}\right)(|\bar{e}_y|^2 + |\bar{e}_x|^2) \\ & + \left(|V_\alpha| + |\tilde{v}_n| + |z_1| + V_x(\tilde{\eta} + \frac{\tilde{\eta}^2}{2})\right)(|\bar{e}_y| + |\bar{e}_x|) \end{aligned} \quad (47)$$

By Proposition 4 the error variable $\tilde{\eta}$ is bounded. For $\dot{V}_5$ to be negative definite the bound of the error of the angle has to satisfy (46). Assuming that this condition is satisfied, it can be shown that the position errors are uniformly bounded and that the nominal system is UPAS. The conditions of Theorem 1 are satisfied and the cascaded system is UPAS on $\boldsymbol{\varphi}_7$.

## VI. Simulation study

In this section we present simulation results, and discuss the performance of the controller.

### A. Simulation setup

The control oriented model (9) with the controllers presented in (11), (18) and (29), was implemented in MATLAB2020B. The analytical expressions for the time derivatives of the attitude reference signal are omitted due to complicated calculations and long expressions. Instead a third order low-pass filter is used to approximate these signals. Incorporating these models into the the analysis is a theoretical gap that might be addressed in future research. The parameters used are given in Table I.

### B. Simulation results.

Figure 2a and 2b show that the USR converges to a desired position along the $x$-axis while oscillating about the desired $y$-position. Note that the amplitude of the oscillations can be reduced or increased by tuning the parameters in $\boldsymbol{\varphi}_7$. This is shown in Figure 2a, where three cases have been plotted with different values for $k$. It is observed that as $k$ increases the amplitude decreases, as expected from the UPAS properties. The path of the USR is shown in Figure 2c. Furthermore, from Figure 2d it can be seen that the norm of the input is bounded. The plot also includes a close up of the input signal, showing that it is continuous and oscillatory. The velocity is seen in Figure 2e, with an excerpt showing that the velocity reaches the reference after approximately $2s$, and although it is UPAS, there is no visible deviation from the desired value. This might be due to either the gain being high or the non-vanishing perturbation $u_\phi$ being low, resulting in a very small deviation from the desired value. The angular velocity, as seen in Figure 2f, is slower and requires roughly $100s$ to reach the desired value. This might be due to the attitude error being dependent on both the velocity and relative joint angle error. These errors are high in the first few time-steps, which might result in the angular velocity deviating. Another reason could be that a low-pass filter is used to approximate the time-derivatives of the reference angular velocity, and it takes time before the output from the low-pass filter becomes a good approximation.

## VII. Conclusions

Previous work has established sufficient conditions for uniform global practical asymptotic stability (UGPAS) and uniform semi-global practical asymptotic stability (USPAS) for nonlinear time-varying dynamical systems and cascaded systems. To the best of our knowledge, there are no results for a local adaptation of these results. Therefore, uniform practical asymptotic stability (UPAS) is defined in this paper and Lyapunov sufficient conditions are provided. Furthermore, it is proven that the UPAS property is retained in cascaded systems.

This is used to design a controller that allows an underwater snake robot (USR) to achieve some desired position in the presence of time-varying disturbances when moving against a constant current along the $x$-axis. The system with the designed controller is proven to be UPAS over the set of parameters. Finally the theoretical results are verified through a simulation study.

## Acknowledgment

This project has received funding from the European Research Council (ERC) under the European Union's Horizon 2020 research and innovation programme, through the ERC Advanced Grant 101017697-CRÈME. The work is also supported by the Research Council of Norway through the Centres of Excellence funding scheme, project No. 223254 – NTNU AMOS and project No. 304667.

## References

[1] E. Kelasidi, P. Liljebäck, K. Y. Pettersen, and J. T. Gravdahl, "Innovation in underwater robots: Biologically inspired swimming snake robots," *IEEE robotics & automation magazine*, vol. 23, no. 1, pp. 44–62, 2016.

[2] C. Bernier, M. Gazzola, R. Ronsse, and P. Chatelain, "Simulations of propelling and energy harvesting articulated bodies via vortex particle-mesh methods," *J. of Computational Physics*, vol. 392, pp. 34–55, Sep 2019.

[3] C. Bernier, M. Gazzola, P. Chatelain, and R. Ronsse, "Numerical simulations and development of drafting strategies for robotic swimmers at low reynolds number," in *Proc. IEEE International Conf. Biomedical Robotics and Biomechatronics*, Enschede, The Netherlands, Aug 2018.

[4] P. Liljebäck, I. U. Haugstuen, and K. Y. Pettersen, "Path following control of planar snake robots using a cascaded approach," *IEEE Transactions on Control Systems Technology*, 2011.

[5] A. M. Kohl, K. Y. Pettersen, E. Kelasidi, and J. T. Gravdahl, "Planar path following of underwater snake robots in the presence of ocean currents," *IEEE Robotics and Automation Letters*, vol. 1, no. 1, pp. 383–390, Jan 2016.

[6] E. Rezapour, A. Hofmann, K. Y. Pettersen, A. Mohammadi, and M. Maggiore, "Virtual holonomic constraint based direction following control of planar snake robots described by a simplified model," in *Proc. IEEE Conf. Control Applications*, Antibes, France, Oct 2014.

[7] M. I. El-Hawwary and M. Maggiore, "Reduction theorems for stability of closed sets with application to backstepping control design," *Automatica*, vol. 49, no. 1, pp. 214–222, Jan 2013.

[8] A. Mohammadi, E. Rezapour, M. Maggiore, and K. Y. Pettersen, "Maneuvering control of planar snake robots using virtual holonomic constraints," *IEEE Transactions on Control Systems Technology*, vol. 24, no. 3, pp. 884–899, may 2016.

[9] A. M. Kohl, K. Y. Pettersen, and J. T. Gravdahl, "Velocity and orientation control of underwater snake robots using absolute velocity feedback," in *IEEE Conf. on Control Technology and Applications*, Maui, HI, Aug 2017.

[10] T. Lee, "Geometric tracking control of the attitude dynamics of a rigid body on SO(3)," in *Proc. American Control Conf.*, San Francisco, CA, Jun 2011.

TABLE I: Simulation parameters

| $N_l$ | $m$ | $c_t$ | $c_n$ | $c_p$ | $\lambda_1$ | $\lambda_2$ | $V_x$ | $V_y$ | $\alpha$ | $\gamma_1(i)$ |
|---|---|---|---|---|---|---|---|---|---|---|
| 10 | 1.56 | 4.45 | 17.3 | 35.7 | 6 | 120 | $-8\ cm/s$ | $-2 * \sin(0.2t)\ cm/s$ | $7\ cm$ | 1 |
| $K_{\phi,1}$ | $K_{\phi,2}$ | $K_{\lambda,1}$ | $K_{\lambda,2}$ | $K_R$ | $K_1$ | $K_2$ | $K_3$ | $k$ | $\delta$ | $\phi_{0,\max}$ |
| 3 | 6 | 2 | 2 | 1 | 2 | 1 | 1 | 0.05 | 40° | 40° |

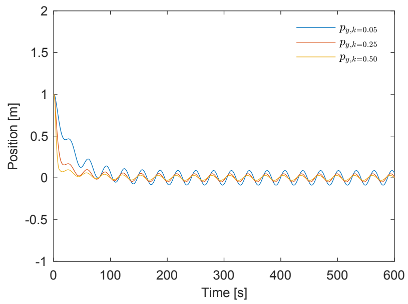


(a) Position along $y$-axis of the USR.

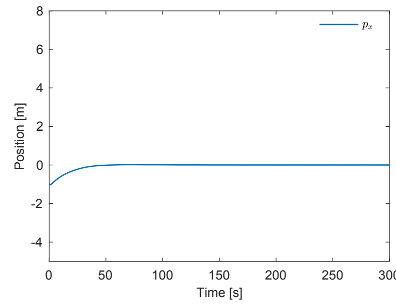


(b) Position along $x$-axis of the USR.

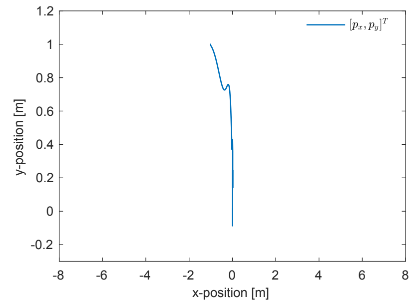


(c) Position of USR.

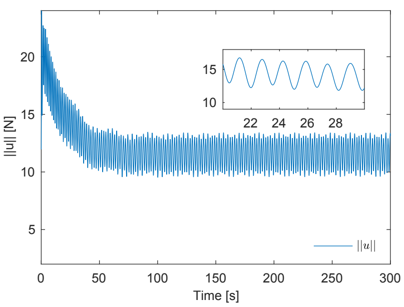


(d) Norm of input.

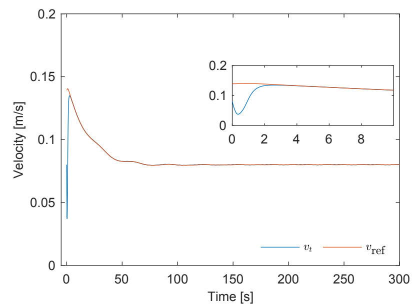


(e) Tangential relative velocity $v_t$ and desired tangential relative velocity $V_d$.

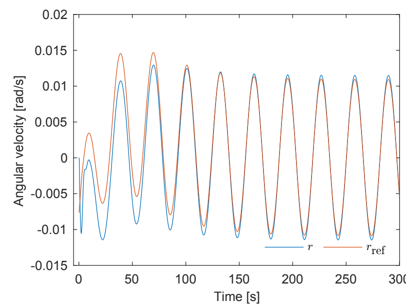


(f) Angular velocity $r$ and desired angular velocity $r_d$.

Fig. 2: Simulation results.


[11] T. Lee, M. Leok, and N. H. McClamroch, "Geometric tracking control of a quadrotor uav on SE (3)," in *Proc. IEEE Conf. decision and control*, Atlanta, GA, Dec 2010.

[12] C. Paliotta and K. Y. Pettersen, "Geometric path following with ocean current estimation for ASVs and AUVs," in *Proc. American Control Conf., Boston, MA*, Oct 2016.

[13] E. Sontag, "Remarks on stabilization and input-to-state stability," in *Proc. IEEE Conf. Decision and Control,*, Tampa, FL, Dec 1989.

[14] E. Panteley and A. Loria, "Growth rate conditions for uniform asymptotic stability of cascaded time-varying systems," *Automatica*, vol. 37, no. 3, pp. 453–460, 2001.

[15] A. Chaillet and A. Loría, "Uniform global practical asymptotic stability for time-varying cascaded systems," *European J. of Control*, vol. 12, no. 6, pp. 595–605, 2006.

[16] M. Vidyasagar, "Decomposition techniques for large-scale systems with nonadditive interactions: Stability and stabilizability," *IEEE Transactions on Automatic Control*, vol. 25, no. 4, pp. 773–779, 1980.

[17] A. Chaillet and A. Loría, "Uniform semiglobal practical asymptotic stability for non-autonomous cascaded systems and applications," *Automatica*, vol. 44, no. 2, pp. 337–347, 2008.

[18] E. Kelasidi, K. Y. Pettersen, J. T. Gravdahl, and P. Liljebäck, "Modeling of underwater snake robots," in *Proc. IEEE International Conf. on Robotics and Automation*, Hong Kong, China, May 2014.

[19] P. Liljebäck, K. Y. Pettersen, Ø. Stavdahl, and J. T. Gravdahl, "Lateral undulation of snake robots: a simplified model and fundamental properties," *Robotica*, vol. 31, no. 7, pp. 1005–1036, Apr 2013.

[20] E. Kelasidi, K. Y. Pettersen, and J. T. Gravdahl, "A control-oriented model of underwater snake robots," in *Proc. IEEE International Conf. Robotics and Biomimetics*, Bali, Indonesia, Dec 2014.

[21] A. M. Kohl, E. Kelasidi, K. Y. Pettersen, and J. T. Gravdahl, "A control-oriented model of underwater snake robots exposed to currents," in *Proc. IEEE Conf. Control Applications*, Sydney, Australia, Sep 2015.

[22] ——, *Sensing and Control for Autonomous Vehicles – Applications to Land, Water and Air Vehicles*. Springer International Publishing, 2017, vol. 474 of Lecture Notes in Control and Information Sciences, ch. Model-Based LOS Path-Following Control of Planar Underwater Snake Robots, pp. 343 – 363.

[23] H. K. Khalil, *Nonlinear systems; 3rd ed.* Prentice-Hall, 2002.

[24] V. I. Arnold, *Mathematical Methods of Classical Mechanics*. Springer New York, 1989.